

Research Article

Seismic performance assessment of timber-framed (himiş) structures with different infill materials

Muhammed Alperen Ozdemir a,* (D)

^a Department of Civil Engineering, Iğdır University, 76000 Iğdır, Türkiye

ABSTRACT

This study investigates the seismic performance of traditional timber-framed (himiş) structures incorporating different types of infill materials through advanced nonlinear finite element modeling. Timber-infilled walls represent a widely used hybrid construction typology in seismic regions, where the interaction between the ductile timber frame and brittle infill materials critically influences structural behavior. Four configurations are analyzed: (1) Timber frame with adobe (mudbrick) infill; (2) Timber frame with fired clay brick infill; (3) Timber frame with natural rubble stone infill; and (4) Bare timber frame. A series of three-dimensional pushover analyses are conducted using ANSYS Workbench, where all materials are modeled using Multilinear Isotropic Hardening plasticity, including contact-based interface definitions and geometric nonlinearity. The mechanical behavior of each wall system is interpreted based on key seismic performance indicators, including initial lateral stiffness, base shear capacity, effective displacement ductility, and energy dissipation. Results show that while infill materials significantly increase the lateral strength and stiffness of the wall systems, they also introduce varying degrees of brittleness and reduced ductility. These findings emphasize the critical role of infill type in the seismic response of timber-framed walls and highlight the importance of understanding frame-infill interaction for the assessment and retrofitting of traditional building stock in earthquake-prone regions.

ARTICLE INFO

Article history:

Received – July 18, 2025
Revision requested – August 11, 2025
Revision received – August 23, 2025
Accepted – September 3, 2025

Keywords:

Timber-framed structures Himiş structures Infill materials Seismic behavior Pushover analysis



This is an open access article distributed under the CC BY licence.

© 2025 by the Author.

Citation: Ozdemir MA (2025). Seismic performance assessment of timber-framed (himiş) structures with different infill materials. Challenge Journal of Structural Mechanics, 11(3), 149–159.

1. Introduction

Timber-framed structures with infill panels—locally known as *himis* in Türkiye—represent a significant segment of the world's vernacular architectural heritage. These hybrid systems, consisting of a load-bearing timber skeleton and non-structural infill walls made from masonry, adobe, stone, or other locally sourced materials, have been used for centuries across a wide variety of climatic, topographic, and seismic regions. Their prevalence is not limited to Anatolia but extends across Europe, Asia, and the Americas, reflecting a universal architectural response to the need for affordable, adaptable, and earthquake-resistant housing.

Timber-framed structures outperform unreinforced masonry buildings during earthquakes primarily due to their light weight, ductile joints, and ability to dissipate seismic energy through controlled deformations. In contrast, masonry walls are typically heavier and brittle, failing suddenly once their limited tensile strength is exceeded. This fundamental difference explains why properly constructed himis systems have repeatedly shown superior survival rates in past earthquakes. In Europe, these systems are widely known under different names: Fachwerk in Germany, Colombage in France, Half-timbering in the United Kingdom, and Pruga or bondruk in the Balkans. Each term denotes a variation of the same core principle: a flexible timber frame, often

^{*} Corresponding author. Tel.: +90-476-223-0040; E-mail address: m.alperen.ozdemir@igdir.edu.tr (M. A. Ozdemir) ISSN: 2149-8024 / DOI: https://doi.org/10.20528/cjsmec.2025.03.004

filled with clay bricks, wattle and daub, or rubble stone. In Asia, similar typologies exist in Japan (*minka*), Nepal and Bhutan (traditional *dzong* buildings), and in the Indian subcontinent under the term *dhajji dewari*, particularly in the Himalayan regions where seismicity is high (Aktaş 2017). In Latin America, the *bahareque* and *quincha* systems in Colombia and Peru, and *taipa de mão* in Brazil, display a comparable structural logic, developed through indigenous knowledge systems that combine seismic intuition with resource economy (Dima and Dutu 2016; Dutu et al. 2018). The global spread of these structures' underscores not only their adaptability to different environments but also their relevance in seismic resilience (Fig. 1). From a structural engineering perspective, the timber frame provides a flexible yet stable

skeleton that accommodates lateral deformations during seismic events, while the infill materials contribute mass and stiffness but may also become sources of vulnerability if poorly integrated. In seismic events such as the 1999 İzmit Earthquake in Türkiye, the 2005 Kashmir Earthquake in Pakistan, the 2015 Gorkha Earthquake in Nepal and the 2023 Kahramanmaraş Earthquakes in Türkiye, observations consistently showed that timberframed structures, when properly constructed, performed significantly better than unreinforced masonry buildings (Vieux-Champagne et al. 2014; Qu et al. 2020; Tan et al. 2024). Their performance is typically characterized by ductile behavior, energy dissipation through joint flexibility, and the ability to localize damage without total collapse.

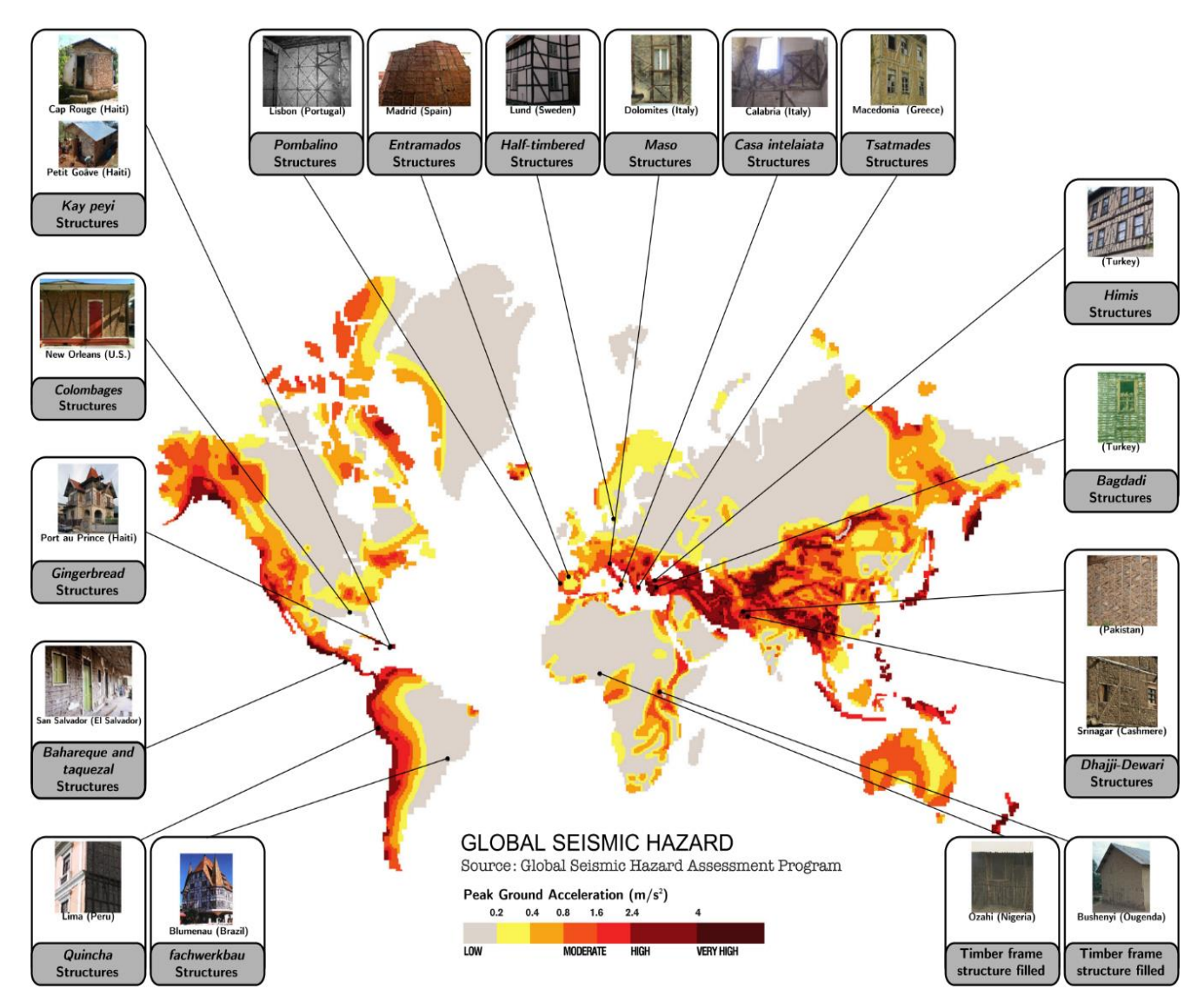


Fig. 1. Examples of the timber-framed structures in the world (Vieux-Champagne et al. 2014).

In addition to their structural role, timber-framed systems with infill panels also offer notable environmental and economic advantages. Locally sourced materials such as timber, adobe, rubble stone, and clay brick reduce transportation needs and embodied energy, contributing to sustainability. These materials are generally

low-cost and easily repairable, which historically made himis construction both affordable and resilient. Recent studies further underline that the ecological footprint of such vernacular materials is significantly lower compared to modern industrial alternatives (Karaman and Zeren 2015; Dikmen 2010).

2. Structural Behavior of the Timber-Framed Structures

In timber-framed wall systems with diagonal bracing and masonry infill, the global lateral stiffness and load-carrying capacity are governed by a combination of axial action in the bracing element, flexural and shear deformation in vertical and horizontal timber members, and in-plane compression of the infill panel. Under in-plane lateral loading, the braced frame with infill may be idealized as a statically indeterminate truss-frame system, where the diagonal brace primarily carries axial forces and the infill behaves as a distributed compression field.

Assuming the brace is pinned at both ends and oriented at an angle θ , the axial force N_b in the brace due to horizontal load P at the top of the wall can be approximated using equilibrium:

$$N_b = \frac{P}{2 \cdot \cos \theta} \tag{1}$$

where, P is the lateral load (e.g., base shear), θ is the angle between brace and horizontal axis and N_b is the axial force in brace.

This force leads to axial deformation in the brace:

$$\delta_b = \frac{N_b \cdot L_b}{A_b \cdot E_b} \tag{2}$$

where, L_b is the length of brace, A_b is the cross-sectional area of brace and E_b is the modulus of elasticity of timber.

The vertical timber elements resist lateral drift through bending. For a cantilever model under lateral top load *P*, the tip displacement due to flexure is:

$$\Delta_{\text{flex}} = \frac{P \cdot h^3}{3EI} \tag{3}$$

Here, Δ_{flex} : Lateral tip displacement due to flexure, P: Lateral load applied at the top, h: Height of the column, E: Modulus of elasticity of timber, I: Moment of inertia of the column cross-section.

The effective lateral stiffness of the system can be idealized as a parallel spring system:

$$K_{\text{total}} = K_{\text{frame}} + K_{\text{brace}} + K_{\text{infill}}$$
 (4)

Here, $K_{\rm frame}$ is the elastic lateral stiffness of the timber frame alone, and $K_{\rm infill,eff}$ is the effective contribution of the infill panel, which depends on its geometry, material stiffness, and contact with the frame. The frame's stiffness can be expressed, for a single-story shear wall, as:

$$K_{\text{frame}} = \frac{12EI}{h^3} \tag{5}$$

Before cracking, the masonry infill panel adds significant stiffness through its in-plane shear and diagonal compression. The initial stiffness of the panel can be approximated using its shear modulus G_m , thickness t, height h, and width b:

$$K_{\text{infill}} = \frac{G_{m} \cdot t \cdot b}{h} \tag{6}$$

$$K_{\text{brace}} = \frac{A_b \cdot E_b}{L_b} \tag{7}$$

where, K_{brace} is the axial stiffness of the diagonal brace, A_b is the cross-sectional area of the brace, E_b is the modulus of elasticity of timber and L_b is the length of the brace.

The lateral resistance from the infill is governed by its compressive strut-like behavior during early loading. However, this capacity rapidly diminishes due to cracking, which can be captured through nonlinear material softening. The energy dissipation potential of the system is closely related to the area under the load–displacement curve:

$$E_d = \int_0^{\Delta_u} P(\Delta) d \tag{8}$$

The ductility ratio μ , which is critical in seismic performance assessment, is defined as:

$$\mu = \frac{\Delta_u}{\Delta_v} \tag{9}$$

where Δ_y is the displacement at yield, and Δ_u is the ultimate displacement at 80% of the maximum lateral load. Higher values of μ indicate greater deformation capacity before collapse.

Contact behavior at the timber–infill interface is another crucial component. The shear resistance at this interface is a function of the friction coefficient μ and the normal contact force N:

$$F_f = \mu \cdot N \tag{10}$$

This governs the onset of sliding and separation, which leads to loss of composite action. Once detachment begins, K_{infill} reduces significantly, and the system behaves similarly to a bare timber frame.

Therefore, the global seismic behavior of timber-framed infilled systems can be understood as a multiphase response:

- Elastic phase: Frame and infill behave monolithically
- Cracking phase: Infill cracks; stiffness decreases
- Plastic/softening phase: Infill loses load-bearing capacity; frame dominates
- Residual phase: Frame sustains remaining loads until failure

3. Finite Element Modeling

This study employs a numerical modeling approach to investigate the seismic performance of traditional timber-framed (himiş) wall systems with various infill materials under lateral earthquake-type loading. The numerical simulations are conducted in a finite element environment using ANSYS Workbench, where nonlinear static (pushover) analyses are performed on three-dimensional wall models. The analysis considers four different wall configurations: (a) A timber frame with adobe (mudbrick) infill; (b) A timber frame with fired clay brick infill; (c) A timber frame with natural rubble stone infill; and (d) A bare timber frame without infill (Fig. 2), used as a reference case to isolate the contribution of infill to the structural behavior.

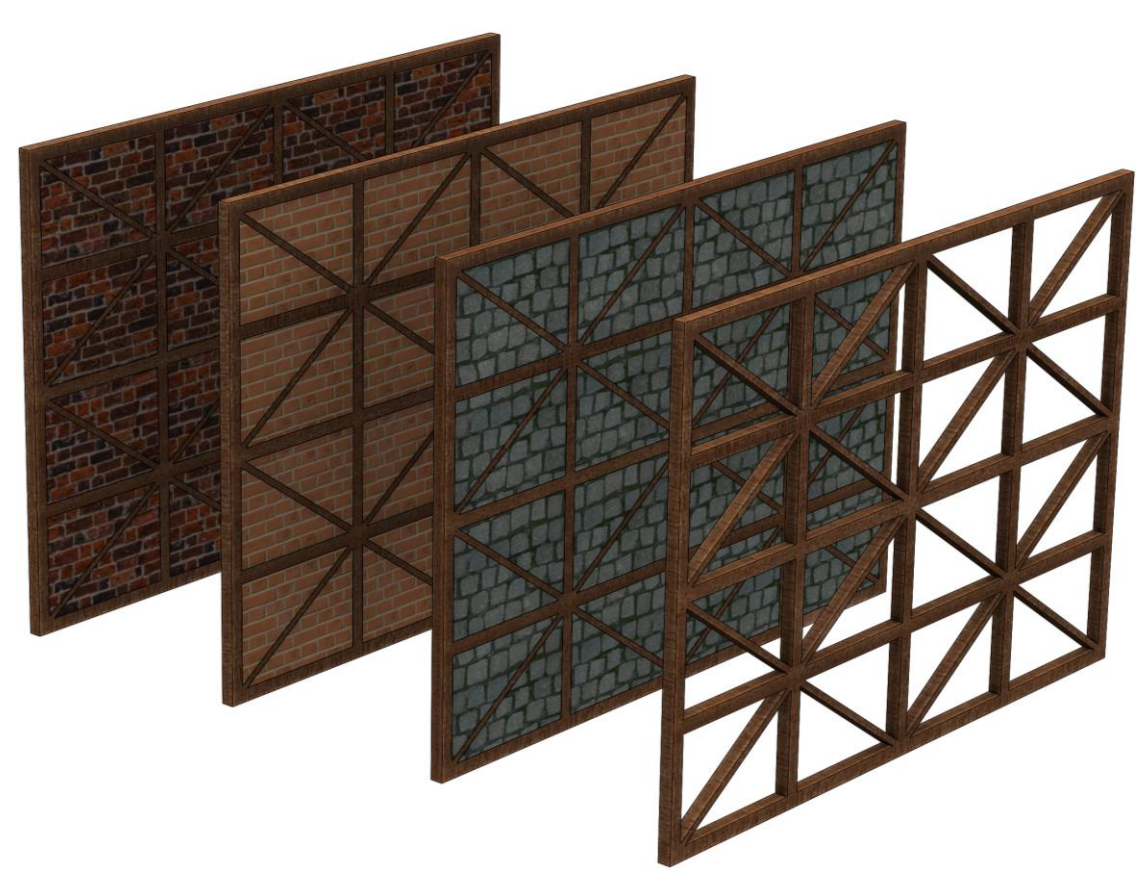


Fig. 2. Different wall configurations: (a) A timber frame with adobe (mudbrick) infill; (b) A timber frame with fired clay brick infill; (c) A timber frame with natural rubble stone infill; and (d) A bare timber frame without infill.

All wall specimens are modeled based on a standardized geometry that reflects traditional himis construction widely observed in Anatolia. The timber framed shear wall has a width of 490 cm and a height of 370 cm, with vertical timber studs spaced at regular intervals and interconnected by horizontal beams and diagonal braces. The cross-sectional dimensions of vertical and

horizontal elements are taken as 10 cm×10 cm while the cross-sectional dimensions of diagonal braces are taken as 10 cm×5 cm, representing typical softwood sections used in himis construction (Fig. 3). The infill is fully enclosed within the timber frame but is not mechanically anchored to it, replicating the friction-based interaction seen in actual historical structures.

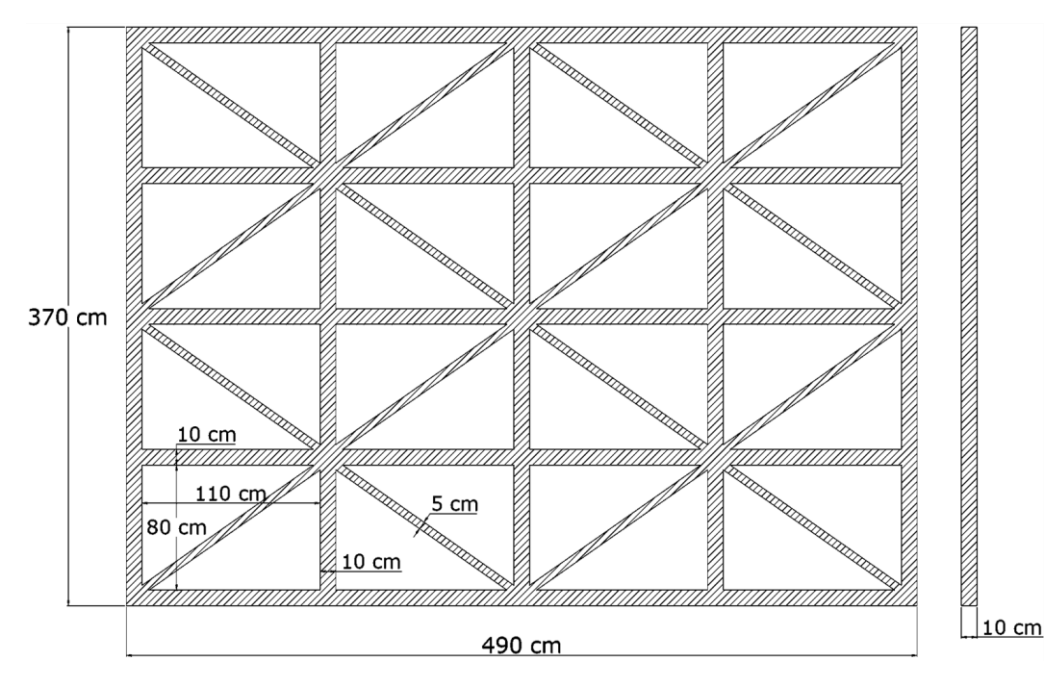


Fig. 3. Dimensions of the timber frame.

The numerical models are developed using SOLID186 elements, which are 20-node hexahedral elements capable of capturing large deformation and plasticity effects. To represent the interaction between the timber frame and the masonry infill, surface-to-surface contact elements (CONTA174 and TARGE170) are employed. Frictional contact is defined as material-dependent coefficients: 0.5 for adobe, 0.4 for fired clay brick, and 0.3 for rubble stone (NAVFAC DM7-02, 1986). Normal separation is allowed, while sliding is governed by a penalty-based Coulomb friction model, enabling the realistic simulation of detachment or slip along the timber-infill interface.

A key feature of this study is the consistent use of the Multilinear Isotropic Hardening (MLIH) plasticity model for all materials, including both the timber and infill types. This modeling choice enables a unified formulation for nonlinear material behavior, while still capturing the distinct stress–strain responses of each material (Table 1). Finite element models (FEMs) of the frames

are given in Fig. 4. The MLIH model was selected for all materials to ensure a unified modeling framework and computational stability. Although timber is orthotropic and masonry materials such as adobe, brick, and rubble stone exhibit brittle fracture modes, adopting a common nonlinear plasticity model allowed for direct comparison between different wall configurations under consistent assumptions. This approach is appropriate for evaluating global seismic performance, although it does not reproduce localized damage mechanisms. While the MLIH plasticity model ensures computational stability and uniformity across different materials, it does not explicitly capture the initiation and propagation of cracks, nor the localization of damage. This simplification is particularly significant for brittle materials such as rubble stone, where fracture and crushing dominate the failure process. Therefore, the results should be interpreted as approximations of global nonlinear response rather than precise simulations of localized cracking behavior.

Table 1. Mechanical properties of materials used in the nonlinear numerical models.

Material	Density (kg/m³)	σ_y (MPa)	E _{initial} (MPa)	Ultimate strain
Timber (pine)	550	30	10,000	0.004
Adobe	1700	1.2	300	0.003
Fired clay brick	1800	10.0	4000	0.0015
Rubble stone	2200	15.0	6000	0.001

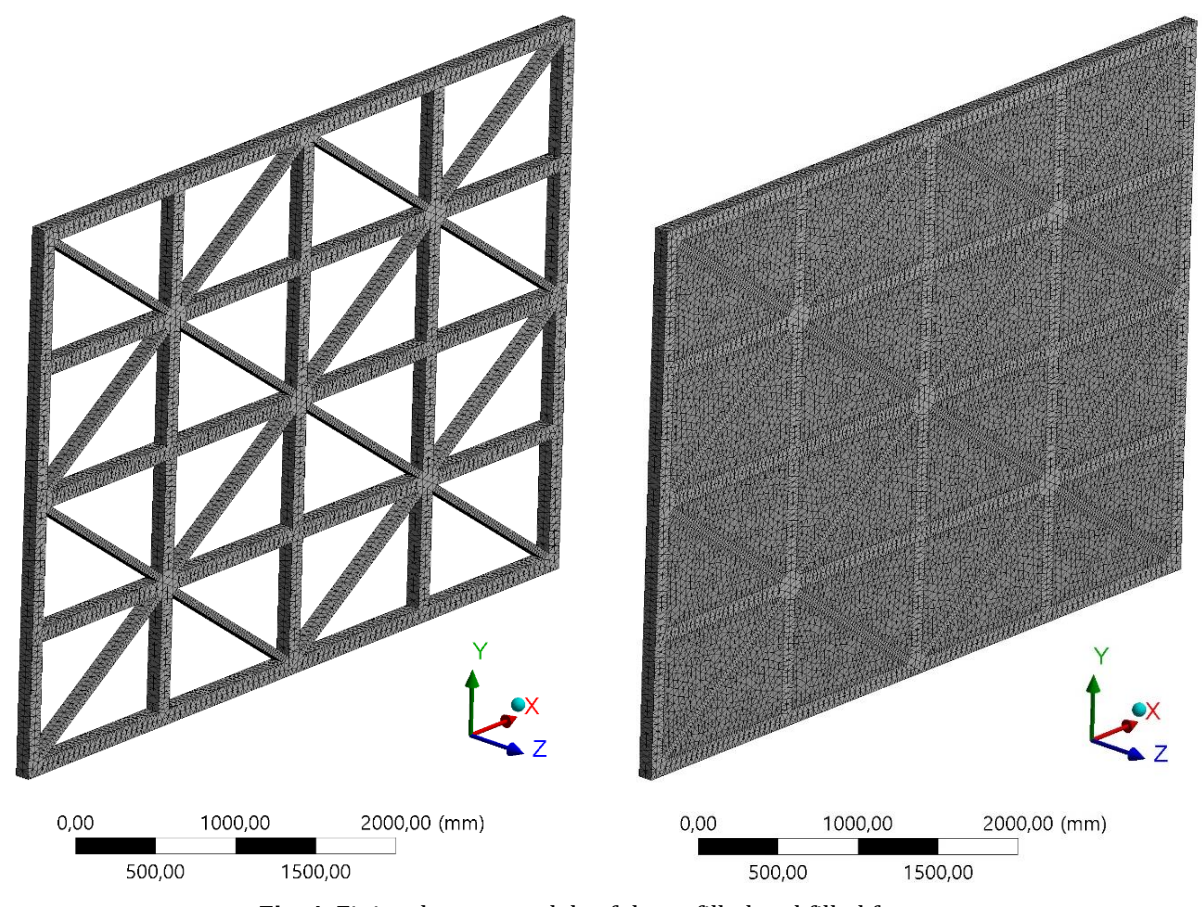


Fig. 4. Finite element models of the unfilled and filled frames.

To ensure reliability of the FEM results, the base of the wall models was fully fixed in all degrees of freedom, while displacement-controlled loading was applied at the top beam to simulate lateral seismic actions. A mesh sensitivity study was conducted, where element sizes were progressively refined until the difference in peak base shear capacity was less than 3%. This confirmed that the selected mesh density provided convergent and mesh-independent results. Convergence was verified in ANSYS through force–displacement equilibrium criteria at each load increment.

4. Pushover Analyses

The pushover analysis is performed under displacement-controlled loading, with a gradually increasing lateral displacement applied at the top beam of the wall. Before lateral loading, self-weight is activated to simulate gravity effects. The base of the wall is fully fixed in all degrees of freedom. The analysis continues until the structure reaches its ultimate capacity and begins to exhibit significant strength degradation or loss of equilibrium. Geometric nonlinearity is included in all analyses to capture large displacement effects, which are particularly relevant for systems with deformable joints and sliding interfaces.

From each simulation, key seismic performance parameters are extracted. These include the initial lateral stiffness, peak base shear, displacement capacity, energy dissipation (measured as the area under the force–displacement curve), and observed failure mechanisms. Special attention is given to the distribution of plastic strain and relative displacement along the timber-infill interfaces, as these are known to influence the global behavior of himis systems. By comparing the capacity curves and ductility of each configuration, the contribution of each infill material to the overall seismic resistance is evaluated.

The methodology adopted herein allows for a controlled comparison of different infill scenarios under consistent boundary and loading conditions, using a computationally efficient and stable material modeling strategy. Although the MLIH model does not capture explicit fracture or crack propagation, it effectively simulates the global nonlinear response and enables meaningful performance assessment of different infill types within timber-framed structures.

The nonlinear pushover analysis provided a clear comparative framework for assessing the seismic performance of the four wall configurations. The force–displacement (capacity) curves obtained from the analysis indicate distinct behavioral patterns for each infill material. Overall, the filled frames exhibited significantly higher lateral stiffness and base shear capacity than the bare timber frame, affirming the structural contribution of the infill panels. However, variations in ductility and energy dissipation behavior among the infill types revealed important trade-offs between strength and deformation capacity.

The rubble stone-infilled frame demonstrated the highest initial stiffness and peak base shear among all

configurations. This is attributed to the high density and compressive strength of stone masonry. However, its capacity curve exhibited a sharp post-peak decline, indicating brittle failure with limited energy dissipation and deformation tolerance. The fired clay brick infill also contributed to considerable stiffness and strength, though to a lesser degree than stone. Its post-peak response was moderately softening, offering a slightly more ductile behavior but still prone to localized interface failure.

The adobe-infilled wall, while having the lowest peak strength among the infilled systems, displayed the most ductile behavior. Its capacity curve showed a gradual softening phase and delayed stiffness degradation, allowing more lateral deformation before failure. This translated into the highest energy dissipation area under the curve and the largest effective ductility ratio. The interface contact in adobe-infilled walls remained engaged longer due to better frictional resistance and more distributed cracking, enabling a more controlled release of seismic energy.

The bare timber frame, as expected, exhibited the lowest strength and stiffness. However, its deformation capacity was considerably high, and no abrupt strength loss was observed even at large lateral displacements. This confirms that in the absence of brittle infill, the timber frame maintains a stable, though flexible, seismic behavior, acting more like a life-safe but damage-prone system.

These behavioral trends are reflected clearly in the following figures (Figs. 5-9). The displacement capacity and energy absorption potential correlate with the postpeak slope and area under each curve, emphasizing the importance of ductility over mere strength. The differences between the configurations highlight the structural and seismic implications of infill material selection in traditional himis walls. The effect of different infill materials on the seismic energy dissipation capacity of timber-framed (himis) structures was investigated in detail. According to the results obtained from pushover analyses, the adobe (mudbrick) infill exhibited the highest energy dissipation capacity with approximately 215.13 kN·m. This was followed by rubble stone infill (113.74 kN·m), fired clay brick infill (27.76 kN·m), and finally the bare frame (4.83 kN·m). The superior performance of adobe can be attributed to its ability to absorb energy through progressive cracking and deformation. Although rubble stone infill had higher strength, its brittle failure mechanism limited its energy dissipation capacity. The brick infill provided moderate performance, while the bare frame exhibited minimal energy absorption due to the absence of lateral stiffness contribution from infill materials. These findings clearly demonstrate that the type of infill material plays a crucial role not only in enhancing load-bearing performance but also in improving the seismic energy absorption and distribution characteristics of the overall structure.

The quantitative results presented in Table 2 high-light the pronounced effect of different infill materials on the seismic behavior of timber-framed (himiş) walls. The bare timber frame exhibited the weakest performance, with an initial stiffness of only 20.57 kN/mm, a maximum base shear of 385 kN, and a ductility ratio of 1.53,

corresponding to an ultimate displacement of 22.8 mm. Its energy dissipation capacity was also minimal (4.83 kN·m), confirming that a timber skeleton alone, without infill, provides inadequate resistance against lateral seismic demands. When adobe (mudbrick) was used as infill, the system demonstrated a moderate increase in strength with $V_{\rm max}$ =908 kN and $K_{\rm initial}$ =38.00 kN/mm,

while achieving a significantly larger ductility ratio (μ =2.50) due to its ultimate displacement of 50 mm. Moreover, adobe exhibited the highest energy dissipation among all configurations (215.13 kN·m), indicating that despite its lower strength, its progressive cracking behavior allows for greater energy absorption and deformation capacity.

Table 2. Seismic performance indicators of timber-framed walls with different infill materials.

Wall configuration	K _{initial} (kN/mm)	V _{max} (kN)	Δ_y (mm)	Δ_u (mm)	$\mu = \Delta_u/\Delta_y$	Energy dissipation (kN.m)
Timber frame + Adobe (mudbrick) infill	38.00	908.0	20.02	50	2.50	215.13
Timber frame + Fired clay brick infill	192.77	3260.9	12.69	50	3.94	27.76
Timber frame + Rubble stone infill	261.60	4345.3	12.46	50	4.01	113.74
Bare timber frame	20.57	385.0	15.04	22.8	1.53	4.83

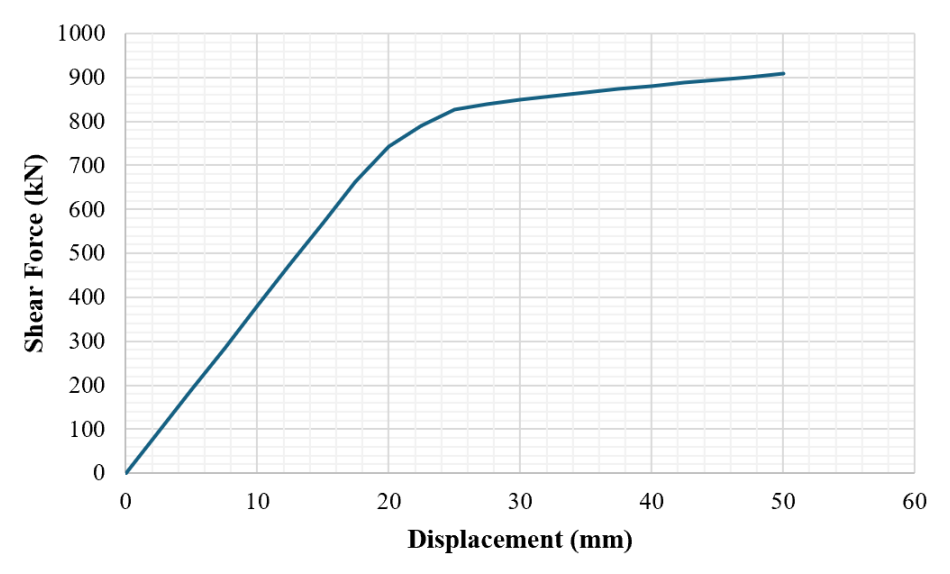


Fig. 5. Pushover curve of the timber frame with adobe (mudbrick) infill.

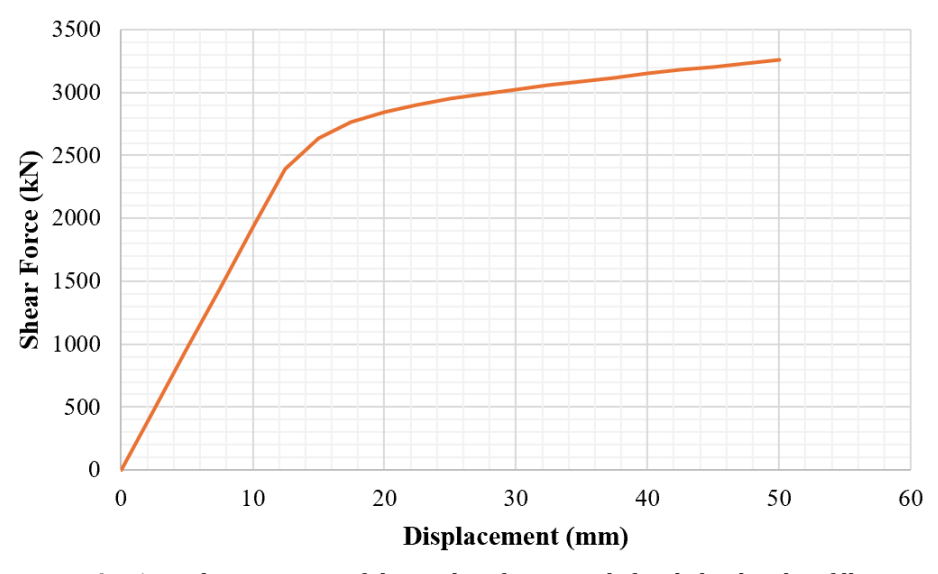


Fig. 6. Pushover curve of the timber frame with fired clay brick infill.

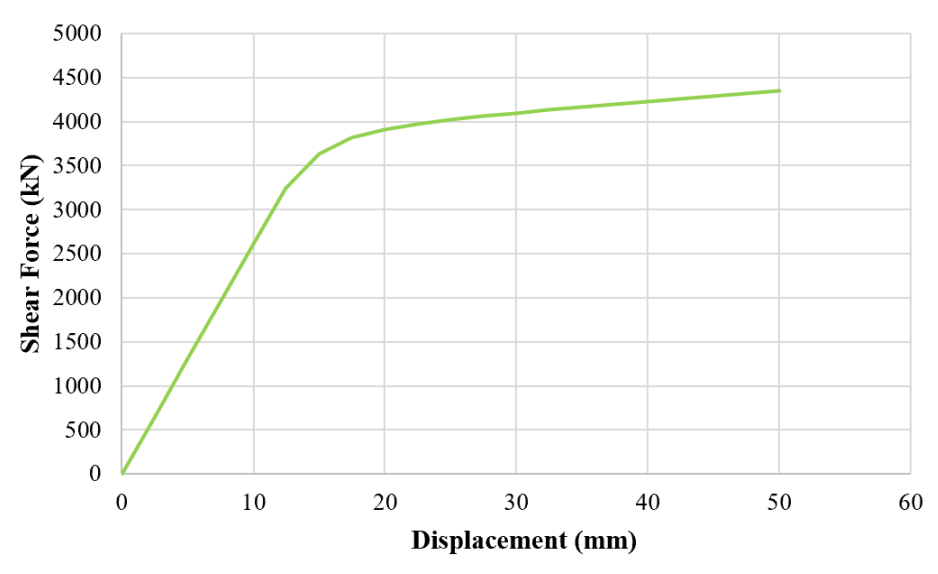


Fig. 7. Pushover curve of the timber frame with natural rubble stone infill.

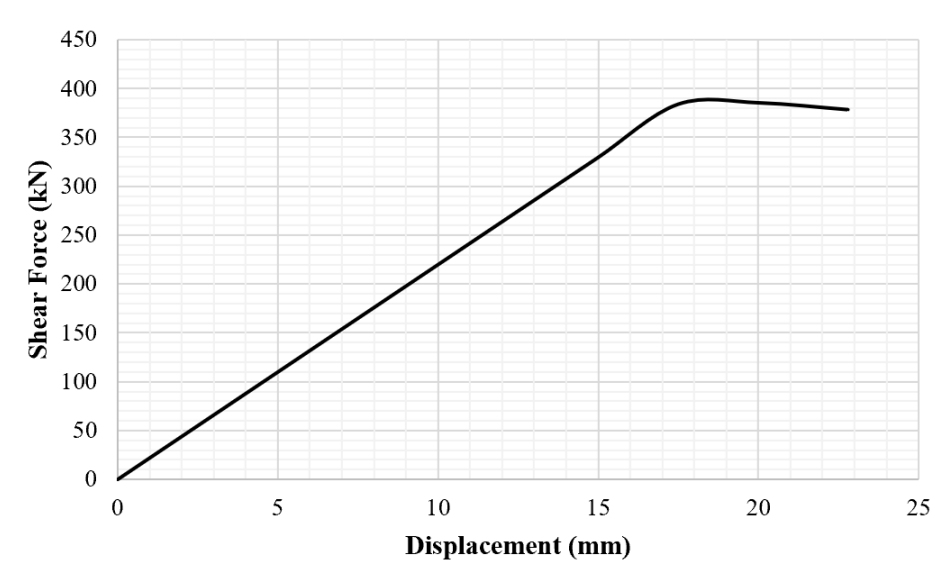


Fig. 8. Pushover curve of the bare timber frame.

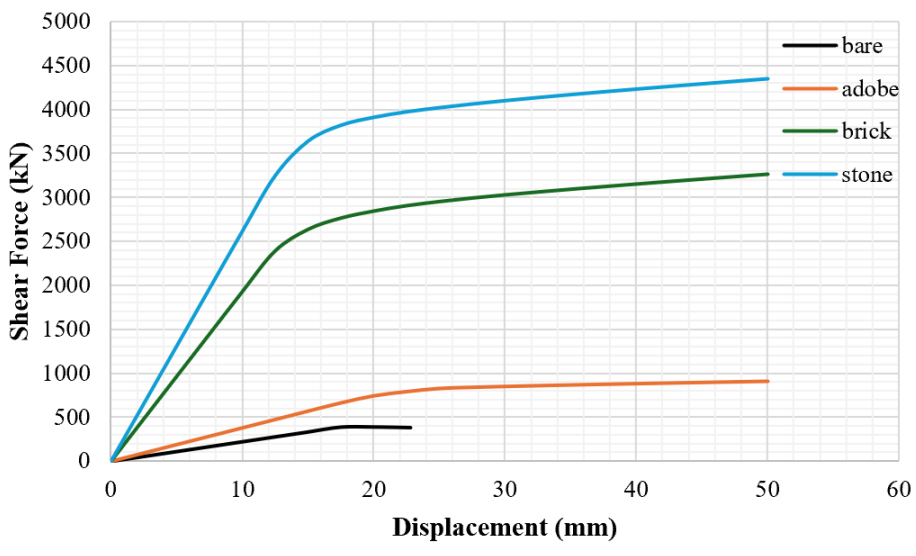


Fig. 9. Force–displacement capacity curves for the wall configurations.

The fired clay brick infill configuration showed a very different pattern. With an initial stiffness of 192.77 kN/mm and a maximum base shear of 3260.9 kN, the brick-infilled wall provided nearly four times the strength of the adobe case (Fig. 10). Its ductility ratio (μ =3.94) was also higher, although the total energy dissipation remained relatively low (27.76 kN·m), pointing to a more brittle failure tendency (Fig. 11). By contrast,

rubble stone infill offered the most balanced seismic performance. It yielded the highest initial stiffness (261.60 kN/mm) and the largest base shear capacity (4345.3 kN), while maintaining a ductility ratio of μ =4.01 with ultimate displacement of 50 mm. Its energy dissipation capacity (113.74 kN·m) was second only to adobe, showing that stone infill can simultaneously provide high strength, stiffness, and considerable energy absorption.

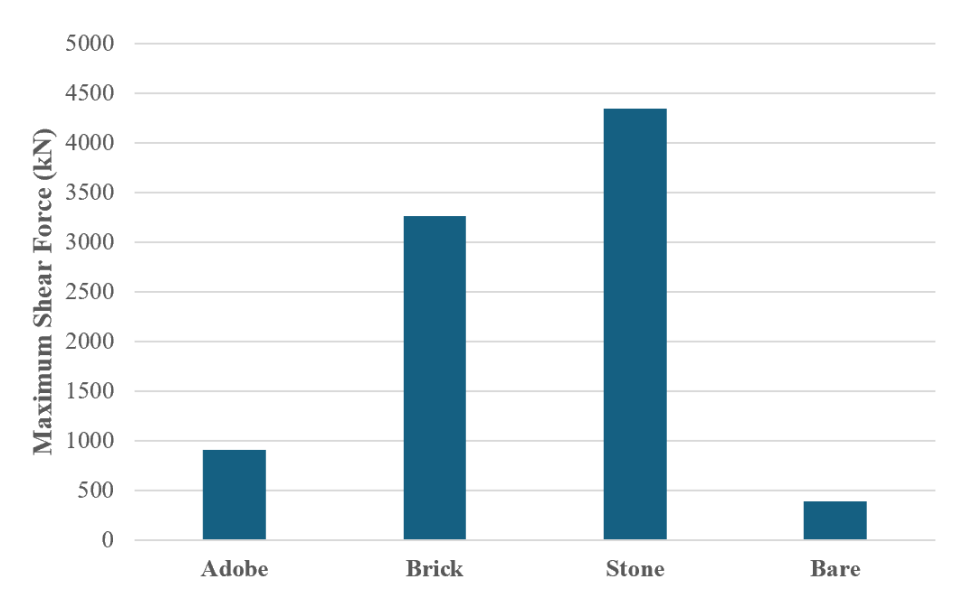


Fig. 10. Maximum shear force results for the wall configurations.

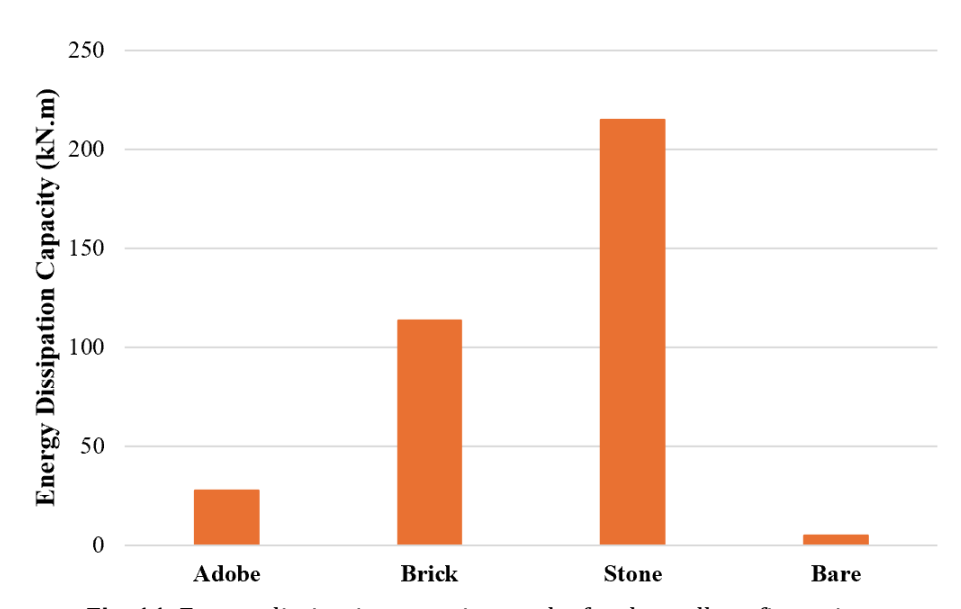


Fig. 11. Energy dissipation capacity results for the wall configurations.

Overall, these findings reveal a distinct trade-off between stiffness and ductility. Adobe infill promotes energy dissipation and ductile behavior but limits lateral strength; fired brick maximizes stiffness and strength at the expense of energy absorption; and rubble stone combines high strength with relatively high ductility, representing the most structurally advantageous configuration. In contrast, the bare timber frame confirms that infill is indispensable for ensuring seismic safety in traditional himis structures.

The failure modes observed in the analyses varied de-

pending on the infill type. In adobe-infilled walls, progressive cracking developed in the panel, while the frame remained engaged until higher drifts, allowing greater ductility. Fired clay brick infill exhibited partial separation at the timber-brick interface, leading to localized sliding and moderate post-peak softening. Rubble stone infill showed brittle crushing and detachment, resulting in a steep strength drop after peak load. In contrast, the bare timber frame exhibited stable but flexible behavior, with deformation concentrated in timber joints and braces (Fig. 12).

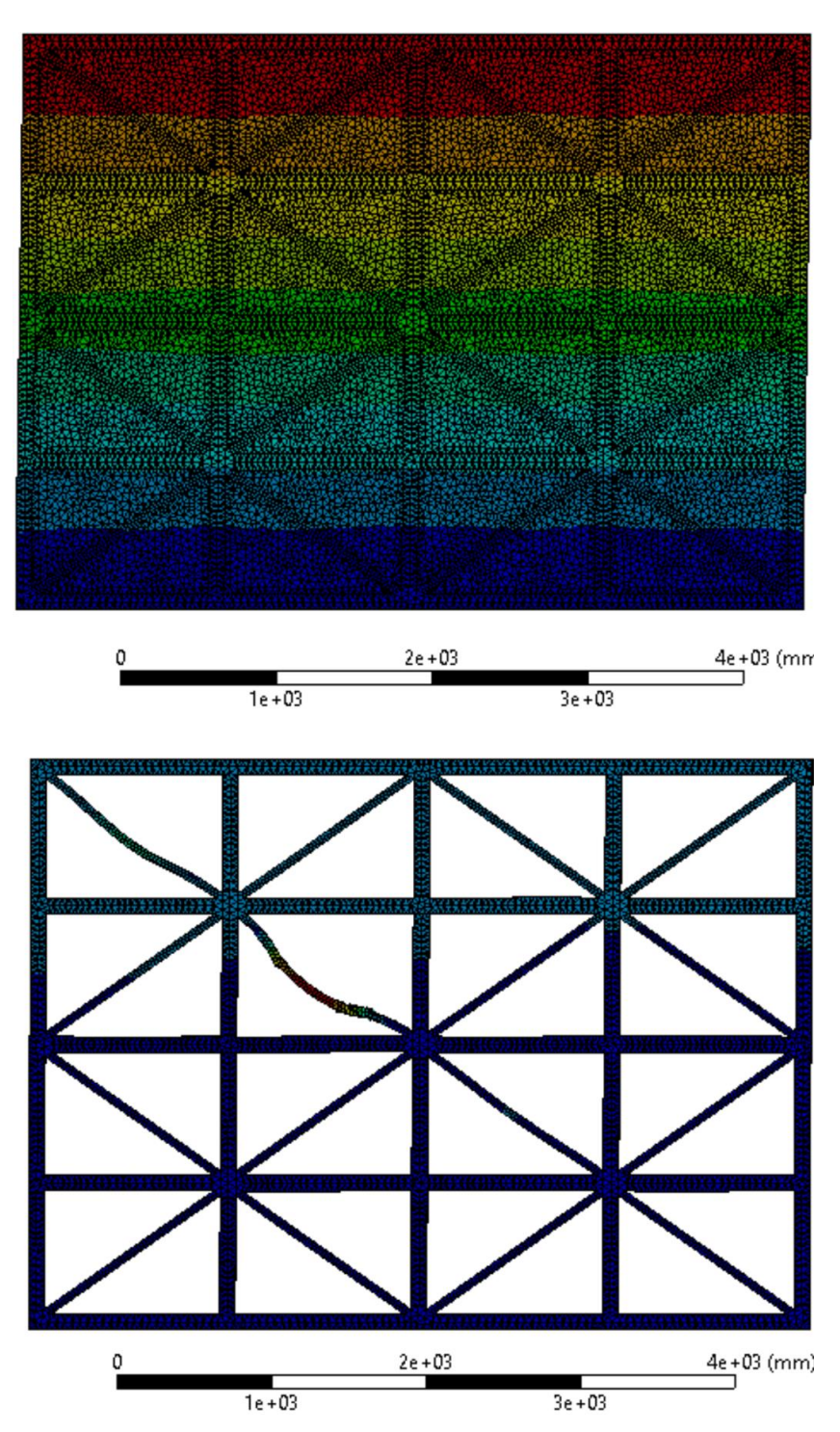


Fig. 12. Structural behavior of the filled and unfilled frames.

5. Conclusions

This study presented a comprehensive seismic performance evaluation of traditional timber-framed (himis) structures with varying infill materials through detailed nonlinear finite element analysis. Four wall configurations were analyzed—bare frame, adobe infill, fired clay brick infill, and rubble stone infill—using 3D pushover analysis in ANSYS Workbench. All materials were modeled with Multilinear Isotropic Hardening plasticity, incorporating frictional contact and geometric nonlinearity to reflect realistic boundary behavior.

The findings revealed that infill materials significantly enhance lateral strength and stiffness but vary widely in terms of ductility and failure mode. Rubble stone provided the highest peak strength but failed in a brittle manner, while fired clay brick offered a more moderate balance between stiffness and ductility. Adobe emerged as the most ductile option, exhibiting high energy dissipation and controlled degradation, making it structurally favorable under large deformations. The bare frame, though weakest, displayed the most stable post-yield behavior and highest drift capacity.

These results underscore the critical influence of infill material properties on the seismic performance of timber-framed systems. In heritage conservation and retrofitting strategies, strength enhancement through infill must be balanced with the need for ductile and energy-dissipating behavior. The numerical framework established in this study allows for effective comparison of different infill typologies under consistent conditions and contributes to the development of performance-based approaches for the preservation and rehabilitation of historic himis buildings in seismic regions.

From a practical perspective, the findings of this study highlight that retrofit strategies for existing himis buildings should carefully consider the choice of infill material. While rubble stone provides higher strength, adobe infill ensures greater ductility and energy dissipation, which is more desirable for seismic safety. In heritage conservation projects, retrofitting approaches should therefore aim not only to strengthen these systems but also to preserve or enhance their ductile performance characteristics.

Acknowledgements

None declared.

Funding

The author received no financial support for the research, authorship, and/or publication of this manuscript.

Conflict of Interest

The author declared no potential conflicts of interest with respect to the research, authorship, and/or publication of this manuscript.

Author Contributions

The author confirms sole responsibility for all aspects of the study including conception and design, acquisition of data, analysis and interpretation of data, drafting the manuscript, revising it critically for important intellectual content; and gave final approval of the version to be published.

Data Availability

The datasets created and/or analyzed during the current study are not publicly available, but are available from the corresponding author upon reasonable request.

REFERENCES

- Aktaş YD (2017). Seismic resistance of traditional timber-frame hımış structures in Turkey: A brief overview. *International Wood Products Journal*, 8(sup1), 21-28.
- Dikmen N (2010). An investigation on traditional timber-framed buildings in Çankırı province of Turkey. *Trakya University Journal of Science*, 11(1), 15-27.
- Dima DI, Dutu A (2016). Traditional buildings with timber frame and various infills in Romania. *Proceedings of the WCTE 2016 World Conference on Timber Engineering*, Vienna, Austria, August 22-25, 1-9
- Dutu A, Niste M, Spatarelu I, Dima DI, Kishiki S (2018b). Seismic evaluation of Romanian traditional buildings with timber frame and mud masonry infills by in-plane static cyclic tests. *Engineering Structures*, 167, 655-670.
- Gani A, Banday JM, Rai DC (2024). Seismic behavior of timber-framed structures infilled with dry brick masonry. *Bulletin of Earthquake Engineering*, 22(13), 6419-6446.
- Karaman ÖY, Zeren MT (2015). Case study: Examples of wooden vernacular architecture Turkish houses in Western Anatolia. YBL Journal of Built Environment, 3(1-2), 77-87.
- NAVFAC DM7-02 (1982). Foundations and Earth Structures. Naval Facilities Engineering Command, Alexandria, VA, USA.
- Qu Z, Fu X, Kishiki S, Cui Y (2020). Behavior of masonry infilled Chuandou timber frames subjected to in-plane cyclic loading. *Engineering Structures*, 211, 110449.
- Tan W, Zhou T, Zhu L, Zhao X, Yu W, Zhang L, Liang Z (2024). Seismic performance of a single-story timber-framed masonry structure strengthened with fiber-reinforced cement mortar. *Materials*, 17(15), 3644.
- Vieux-Champagne F, Sieffert Y, Grange S, Polastri A, Ceccotti A, Daudeville L (2014). Experimental analysis of seismic resistance of timber-framed structures with stones and earth infill. *Engineering Structures*, 69, 102-115.